

Layer-Specific Scaling of Positional Encodings for Superior Long-Context Modeling

Zhenghua Wang^{*1,3}, Yiran Ding^{*2}, Changze Lv^{*1,3}, Zhibo Xu^{1,3}, Tianlong Li^{1,3}, Tianyuan Shi^{1,3}, Xiaoqing Zheng^{†1,3}, Xuanjing Huang^{1,3}

¹Fudan University ²Westlake University

³Shanghai Key Laboratory of Intelligent Information Processing

{zhenghuawang23, czlv24}@m.fudan.edu.cn, {yiran.ding}@hdu.edu.cn
{zhengxq, xjhuang}@fudan.edu.cn

Abstract

Although large language models (LLMs) have achieved significant progress in handling long-context inputs, they still suffer from the “lost-in-the-middle” problem, where crucial information in the middle of the context is often underrepresented or lost. Our extensive experiments reveal that this issue may arise from the rapid long-term decay in Rotary Position Embedding (RoPE). To address this problem, we propose a layer-specific positional encoding scaling method that assigns distinct scaling factors to each layer, slowing down the decay rate caused by RoPE to make the model pay more attention to the middle context. A specially designed genetic algorithm is employed to efficiently select the optimal scaling factors for each layer by incorporating Bézier curves to reduce the search space. Through comprehensive experimentation, we demonstrate that our method significantly alleviates the “lost-in-the-middle” problem. Our approach results in an average accuracy improvement of up to 20% on the Key-Value Retrieval dataset. Furthermore, we show that layer-specific interpolation, as opposed to uniform interpolation across all layers, enhances the model’s extrapolation capabilities when combined with PI and Dynamic-NTK positional encoding schemes.

1 Introduction

Recent advancements in long-context LLMs (Team et al., 2024; Dubey et al., 2024; Liu et al., 2024a) have attracted considerable attention, enabling these models to process longer inputs and tackle more complex tasks, such as long-text summarization (Feng et al., 2021; Zhang et al., 2021), long-context question-answering (Li et al., 2024b), and advanced code generation (Zheng et al., 2023; Liu et al., 2024b). However, as the context length increases, these models encounter the “lost-in-the-middle” problem (Liu et al., 2024c; Li et al., 2023),

^{*}Equal Contribution

[†]Corresponding Author

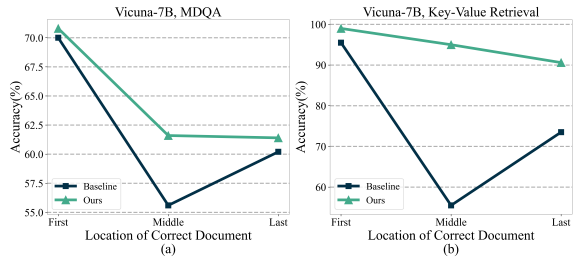


Figure 1: Average accuracy on MDQA (a) and the Key-Value Retrieval (b) datasets. By applying layer-specific scaling to enhance middle-context attention, we achieved an average accuracy improvement of +20% on the Key-Value Retrieval dataset and +2.7% on the MDQA dataset.

where they disproportionately focus on the beginning and end of the context while overlooking critical information in the middle. This issue can substantially degrade performance across various long-context tasks.

RoPE is a widely used positional encoding in Transformer-based LLMs, designed to capture relative distances between input tokens while gradually reducing inter-token dependencies as the distance increases (Su et al., 2024). Recent studies suggest that this long-term decay effect may contribute to the “lost-in-the-middle” problem. To address this, Zhang et al. (2024) proposes assigning different scaling factors to attention heads based on their sensitivity to relevant information. However, this approach has three key shortcomings:

- I. Although scaling factors are dynamically assigned based on the properties of each attention head, they are applied within the same range across all layers, which may fail to account for layer-specific variations (Li et al., 2024a; Men et al., 2024; Sun et al., 2024).
- II. There is no systematic approach that generalizes across different models and datasets for effectively determining the optimal range of scaling factors.

III. During inference, this method requires computing each attention head’s sensitivity to relevant information to determine its scaling factor. This incurs additional time overhead, resulting in prolonged response times. In contrast, our approach eliminates this burden, maintaining efficiency while enhancing model performance.

Additionally, preliminary experiments indicate that a uniform scaling strategy that assigns the same scaling factors across all layers and heads can alleviate the “lost-in-the-middle” problem. However, it introduces a new issue: “lost-in-the-tail”, where the model’s ability to capture information at the end of input texts is weakened. To address the limitations mentioned above, we seek to assign distinct scaling factors to each layer, as our findings suggest that scaling different layers yields varying effects, as showing in Table 4.

Determining appropriate scaling factors for each layer is challenging. Assuming that the appropriate scaling factor for each layer is selected from a finite set of scaling factors, as each layer can have multiple choices, leading to a rapidly expanding combinatorial optimization problem as the number of layers increases. To address this, we apply a genetic algorithm to solve the optimization problem, limiting the search space to Bézier curves which approximately boosts search speed by a factor of 10^{20} over brute-force search across 32 layers. A Bézier curve, defined by a small number of key points, is used to model the functional relationship between scaling factors and layer depths. By selecting these points, we can determine the corresponding Bézier curve and, consequently, the scaling factors for each layer.

By combining the specially designed genetic algorithm with Bézier curves, we can optimize layer-specific scaling factors efficiently, typically within 4 to 8 hours, using a modest amount of computational resources. For instance, the appropriate layer-specific scaling factors for the Vicuna-7B-v1.5 model (Berkeley et al., 2023) can be determined in just 6 hours using four A100 GPUs on the MDQA dataset (Liu et al., 2024d). Given the significant improvements in long-context modeling for LLMs, investing a few hours and some computational resources to select the optimal layer-specific scaling factors is a worthwhile trade-off.

The contributions of this study can be summarized as follows.

- We propose a layer-specific positional encod-

ing scaling method that effectively alleviates the “lost-in-the-middle” problem, thereby enhancing the model’s ability to handle long-context tasks. Furthermore, this approach is highly versatile and can be applied to a wide range of models.

- We propose an efficient and fast genetic search algorithm, where the search space is constrained by Bézier curves, enabling the rapid determination of the scaling factors for each layer using only a few representative examples.
- We investigate the underlying causes of the “lost-in-the-middle” problem and offer a reasonable explanation for why our layer-specific positional encoding scaling method can effectively mitigate this problem.

2 Related Work

2.1 Positional Encoding

Positional encoding can be categorized into two main types: absolute positional encoding (Clark et al., 2020; Lan et al., 2019) and relative positional encoding (Su et al., 2021; Huang et al., 2020; Shaw et al., 2018). Absolute positional encoding directly adds the absolute positional information to token embedding, while relative positional encoding models the relative distance between tokens. In relative positional encoding, RoPE has become a mainstream method due to its excellent extrapolation property and adaptability to linear attention.

With RoPE (Su et al., 2021), the relative positional relationships are reflected through the dot product operation:

$$f(\mathbf{q}_m, m)^T f(\mathbf{k}_n, n) = g(\mathbf{q}_m, \mathbf{k}_n, m - n) \quad (1)$$

The function f represents the rotation of the query vector q at position m and the key vector k at position n , incorporating positional information into them. The dot product of the rotated vectors reflects the relative position $m - n$.

Position interpolation (PI) (Chen et al., 2023a) expands the context window by narrowing the interval between position indices. The RoPE function f is replaced by f' defined as follows:

$$f'(x, m) = f(x, \frac{m}{s}) \quad (2)$$

$$s = \frac{L'}{L}$$

where L is pretrained context window size of the LLMs and L' is the extended context window size,

and m is the position index. PI scales the original relative distance by a factor of $\frac{1}{s}$.

2.2 The Lost-in-the-Middle Phenomenon

The “lost-in-the-middle” issue is a prevalent challenge in both open-source and closed-source models (Liu et al., 2024c). This issue arises when critical information is positioned in the middle of the model’s context, causing the model to struggle with effectively processing and understanding the content, which ultimately results in a performance decline. Recent approaches to mitigate this problem can be broadly categorized into three types: fine-tuning-based methods, positional encoding-based methods, and attention-based methods.

In fine-tuning-based methods, He et al. (2024); An et al. (2024) propose constructing a dataset that emphasizes information located in the middle positions. By applying instruction fine-tuning, the model can be guided to pay more attention to the central part of the context. However, this approach requires considerable human effort to curate the relevant samples and entails substantial computational costs for the fine-tuning process. In positional encoding-based methods, the primary approach is to interpolate RoPE to mitigate long-term decay, enabling the model to better focus on information in the middle of the context. Zhang et al. (2024) performs interpolation at the head level of multi-head attention, while Chen et al. (2023b) applies interpolation at the model level, where multiple models with different scaling factors run in parallel and decode the next token based on confidence scores. However, both methods introduce substantial time and memory overhead. In attention-based methods, Peysakhovich and Lerer (2023) reposition relevant documents to areas of the context where the model’s attention is most concentrated, based on attention weights. Hsieh et al. (2024) formulates a positional bias equation, rescaling the attention score matrix to address the model’s bias toward specific positions.

2.3 Bézier Curve

Bézier curves are parametric curves widely utilized in computer graphics and related fields (Mortenson, 1999). They are defined by a set of control points, which generate a smooth and continuous curve through a mathematical formula. The defining feature of Bézier curves is that a small number of control points can precisely shape complex curves, making them especially valuable in applica-

tions such as automotive body design (Mineur et al., 1998; Zheng et al., 2020), font creation (Haryono, 2014), and animation (Bargteil and Cohen, 2014)

A Bézier curve of degree n is defined as:

$$B(t) = \sum_{i=0}^n B_i P_i \quad (3)$$

where P_i are the control points, B_i are the Bernstein basis polynomials given by:

$$B_i^n(t) = \binom{n}{i} (1-t)^{n-i} t^i, \quad t \in [0, 1] \quad (4)$$

where $\binom{n}{i}$ is the **binomial coefficient**:

$$\binom{n}{i} = \frac{n!}{i!(n-i)!} \quad (5)$$

3 Method

In this section, we first conduct experiments to validate the potential causes of the “lost-in-the-middle” phenomenon and establish the rationale for layer-specific positional encoding scaling(§3.1). Next, we formally define the problem using mathematical formulations, aiming to enhance the model’s ability to utilize middle-position information without degrading its original performance(§3.2). Finally, we present a detailed methodology for assigning optimal scaling factors to each layer, leveraging a combination of genetic algorithms and Bézier curves(§3.3). The overall workflow is represented in Figure 2.

3.1 Layer-Specific Scaling Enhanced Context Utilization

The “lost-in-the-middle” phenomenon causes the model to focus more on the ends of the context while neglecting the middle information, which may be due to the following two reasons:

(1) Causal Attention Mechanism: The causal attention mechanism causes the model to focus more on the beginning of the sequence, as earlier tokens are involved in more attention calculations. To investigate the effect of causal attention, we use the **Vicuna-7B-v1.5** (Berkeley et al., 2023) and **LLaMA-2-7B-hf** (Touvron et al., 2023) to conduct experiment on the **QMSum** dataset (Shaham et al., 2023). We randomly sample 50 items from the dataset and remove the RoPE from layers 2 to 4. Then, we extract the hidden states from layer 4 and calculate the average cosine similarity between the mean representations of the first 128 tokens and representations of the subsequent tokens. As shown in

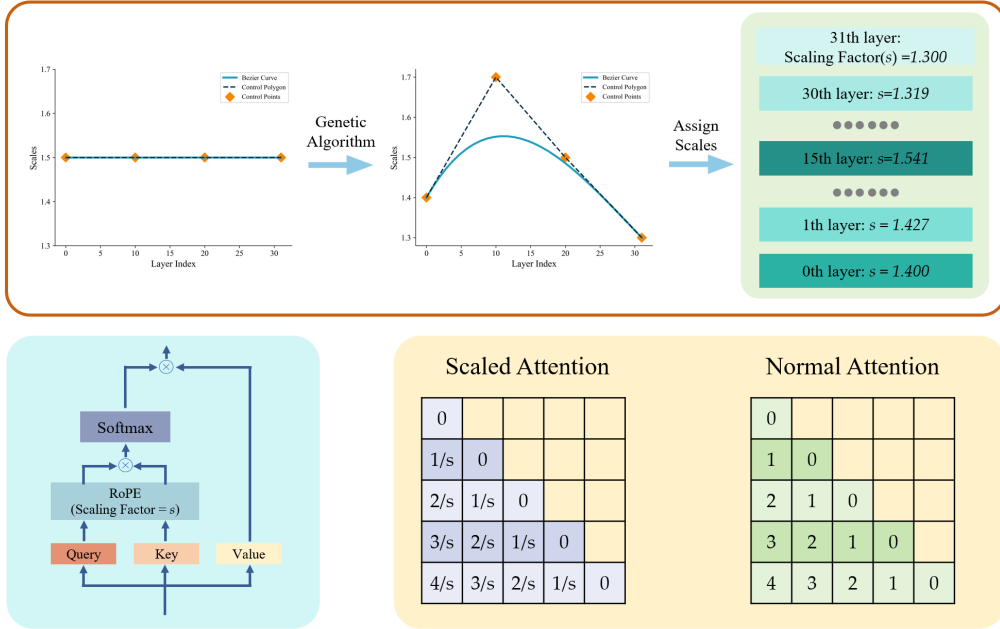


Figure 2: **Modeling with Bézier Curves:** First, we optimize the initial control points to optimal points using a constrained genetic algorithm. Then, we apply scaling factors derived from the fitted curve to each layer. The bottom part of the figure illustrates the model structure, alongside a comparison between the scaled attention and the normal attention.

Figure 3, the representations of later tokens become more similar to those of earlier tokens in the absence of RoPE, which is the opposite of the normal trend. This demonstrates that the model’s causal attention makes it focus more on earlier content.

(2) Long-term decay of RoPE: The Long-term decay of RoPE causes the model to focus more on the end of the sequence. As the relative distance increases, the attention scores decay rapidly, leading the model to focus excessively on nearby tokens during autoregressive decoding, while neglecting information from distant tokens. We scale the RoPE by a factor of s , reducing the relative distance to $1/s$ of its original value. This alleviates the decay rate as shown in Figure 4, allowing the model to focus not only on nearby tokens but also on more distant tokens, particularly those in the middle positions. Adopting the experimental setup described previously, additionally, we partitioned the context into three parts and calculated the cosine similarity between the average representation of the middle part tokens and the representation of the last token at different scales. As the scale increases, the similarity between representations improves which is shown in Figure 5, demonstrating that scaling RoPE allows the model to focus more on the content of the middle part during autoregressive decoding.

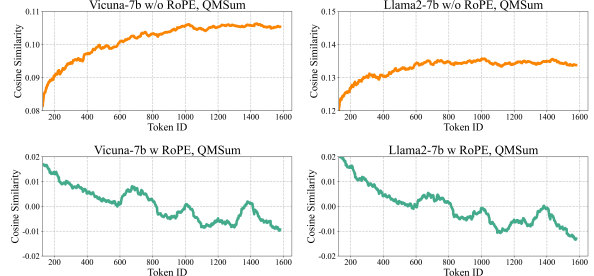


Figure 3: Cosine similarity between the average of first 128 tokens and the later tokens reveals the model heightened focus on earlier content without positional encoding.

To mitigate the “lost-in-the-middle” problem, we have two options: shift excessive attention from the start of the context to the middle positions or redistribute attention from the end of the context. Given that causal attention is a fundamental part of the model’s architecture and is difficult to modify, we opted for the latter. As depicted in the bottom of Figure 2 and in Figure 4, we redistribute attention from the later part to the middle part by scaling RoPE.

Applying uniformly large scaling factors to layers can ease the “lost-in-the-middle” problem, yet it may neglect the content at the end position (Zhang et al., 2024). We suggest applying scaling factors to specific layers, as shown in Table 4, to enhance

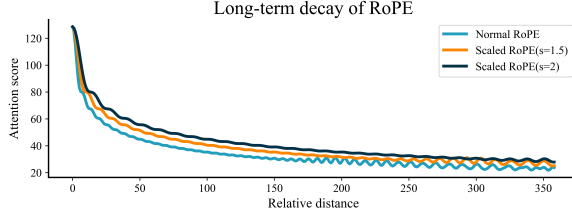


Figure 4: The rapid decay of RoPE biases local focus, while the scaling operation can slow the decay, contributing to the enhancement of global attention capacity.

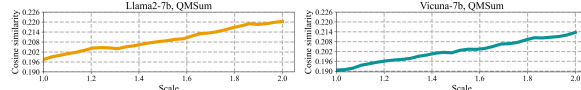


Figure 5: Cosine similarity between the average of middle context and the last token reveals the model heightened focus on middle context as the scaling factor increases.

the model’s utilization of the end part context. Our findings indicate that scaling earlier layers likely improves the model’s comprehension of the context’s ending part while scaling later layers tends to enhance its understanding of the context’s beginning part. Therefore, we should dynamically assign scaling factors to layers based on their characteristics.

3.2 Problem Formulation

To efficiently determine the optimal scaling factors for each layer, we employ the Bézier curve to model the functional relationship between layer depths and scaling factors. Subsequently, a genetic algorithm is applied to determine the control points of the curve. Given the model parameters θ and the dataset X , our goal is to boost the model’s exploitation of context at middle positions while ensuring that the performance at both ends of the context does not degrade. This goal can be formulated as follows:

$$\arg \min_{\mathbf{S}; s_i \geq 1} \mathbb{E} \left[\sum_{x \in \mathbf{X}} \mathcal{L}(x, \text{LLM}(\theta, \mathbf{S})) \right] \quad (6)$$

S is the set of scaling factors for each layer of the model. To slow the long-term decay phenomenon and prevent harm to the model’s context window, each element s_i in the set is greater than 1, as shown in Figure 4. **LLM** is a function that scales the positional encoding of the model’s layers according to the set S .

$$\mathbf{S} = B(t), \quad t \in \left\{ \frac{k}{n} \mid k = 0, 1, 2, \dots, n \right\} \quad (7)$$

n is the number of layers that will be scaled. Since the value of t ranges from 0 to 1, we divide t into equal intervals according to the number of layers.

3.3 Searching the Layer-Specific Scaling Factors

Brute-force search is impractical for determining the scaling factors for each layer due to its complex search space. Therefore, we employ a genetic algorithm to determine the control points of Bézier curves.

Search space: We follow Ding et al. (2024), discretizing the continuous search space to enable more efficient searching. Assume the control points of the Bézier curve are (B_x, B_y) , where $B_x \in [0, n - 1]$ (n is the number of layers) and $B_y \in [1, 2]$. The values of B_x are discretized with a step size of 1, and the values of B_y are discretized with a step size of 0.1 which is represented in table 1. Assuming the model consists of 32 layers and the scaling factor for each layer is determined from the B_Y set, the total number of choices for a brute-force search is 11^{32} . If a Cubic Bezier curve is used, each control point has $32 * 11$ possible combinations. With four control points, the total search space is 352^4 which approximately narrows the search space by a significant factor 10^{20} compared to brute-force search.

	Search Space
B_X	$\{0, 1, 2, 3, 4, 5, 6, 7, 8, \dots, n - 4, n - 3, n - 2, n - 1\}$
B_Y	$\{1.0, 1.1, 1.2, 1.3, 1.4, 1.5, 1.6, 1.7, 1.8, 1.9, 2.0\}$

Table 1: Search space for the control point of Bézier curves.

Genetic algorithm: We use a Cubic Bezier curve with four control points to conduct the following experimental analysis. The first individual is initialized as follows:

$$\mathbf{P} = \left[\left(\frac{(n-1) \cdot i}{3}, 1.5 \right) \mid i = 0, 1, 2, 3 \right], \quad (8)$$

where n is the number of scaling layers, based on the experimental setup of Zhang et al. (2024), we set the B_y of all control points to 1.5. The remaining individuals from the population will undergo mutations based on the first individual.

To ensure the stability and effectiveness of the search algorithm, the following constraints were applied to the mutation and crossover operations:

- (1) The B_x of all control points are increasing monotonically to ensure the smoothness of the

Algorithm 1 The search algorithm for determining layer-specific scaling factors

Input: target LLM, input samples \mathbf{X} , population size P , mutation size N_1 , crossover size N_2 , max iterations \mathcal{T} , mutate probability p

- 1: Top-k= ϕ ;
- 2: $P_0 = \text{Initialize_population}(P, \mathbf{X}, p)$;
- 3: **for** $i=1$ to \mathcal{T} **do**
- 4: **Compute_context_utilization** (LLM, P_{i-1} , \mathbf{X});
- 5: Top-k = **Update_Topk** (Top-k, P_{i-1});
- 6: $P_{\text{mutation}} = \text{Mutation_with_constraint}$ (Top-k, N_1 , p);
- 7: $P_{\text{crossover}} = \text{Crossover_with_constraint}$ (Top-k, N_2);
- 8: $P_i = P_{\text{mutation}} \cup P_{\text{crossover}} \cup \text{Top-k}$;
- 9: **end for**
- 10: Return the individual with highest context utilization in Top-k;

curve to prevent abrupt changes in scaling factors. Let B_x^j and B_x^i denote the first dimension of the j -th and i -th control points, respectively. The relationship between them is as follows:

$$0 \leq B_x^j < B_x^i \leq n - 1 \quad \text{if } i > j \quad (9)$$

(2) the mutation operation modifies B_x and B_y within a specific range to prevent excessive curve variations to avoid affecting the convergence stability of the search. Let N_x denote the amplitude of change in the first dimension(layer index), and N_y denote the amplitude of change in the second dimension(Scaling factor), n represent the number of layers.

$$\begin{aligned} \hat{B}_x^i &= \begin{cases} [\min(0, B_x^i - N_x), \max(B_x^{i+1}, B_x^i + N_x)] & \text{if } i = 0, \\ [\min(B_x^{i-1}, B_x^i - N_x), \max(B_x^{i+1}, B_x^i + N_x)] & \text{if } i \in (0, k), \\ [\min(B_x^{i-1}, B_x^i - N_x), \max(B_x^i + N_x, n - 1)] & \text{if } i = k. \end{cases} \\ \hat{B}_y^i &= \begin{cases} [\min(1, B_y^i - N_y), \max(B_y^i + N_y, 2)] & \text{if } i = 0, \\ [\min(1, B_y^i - N_y), \max(B_y^i + N_y, 2)] & \text{if } i \in (0, k), \\ [\min(1, B_y^i - N_y), \max(B_y^i + N_y, 2)] & \text{if } i = k. \end{cases} \end{aligned} \quad (10)$$

Algorithm 1 formalizes the multi-objective optimization for layer-adaptive scaling factors. The function **Compute_context_utilization** is defined as a \mathcal{U} .

$$\mathcal{U} = \lambda_f A_f + \lambda_m A_m + \lambda_l A_l \quad (11)$$

where A_f, A_m, A_l denote accuracy when target documents appear in first/middle/last context positions, with constraint weights $\lambda_f, \lambda_m, \lambda_l \in \mathbb{R}^+$. To prevent degradation of last context utilization, we enforce monotonic weight ordering:

$$\lambda_f < \lambda_m < \lambda_l \quad (12)$$

The operation **Crossover_with_constraint** will swap the control points between two individuals with a certain probability. However, any changes

made during the crossover process must satisfy the constrain Equation (9). If the modified crossover does not meet the constrain Equation (9), a new pair of individuals will be selected again for crossover. The maximum retry number of crossover is set $2N_2$, in order to prevent situations where no valid crossover individuals are found.

4 Experiment

In this section, we demonstrate that the layer-specific positional encoding scaling effectively mitigates the “lost-in-the-middle” problem and enhances the model’s ability to utilize contextual information(§4.1). Moreover, compared to uniform scaled positional encoding , this method demonstrates superior performance in enhancing the model’s extrapolation capability(§4.2).

4.1 Enhanced Ability to Utilize Contextual Information

Experimental Setup We selected three mainstream RoPE-based LLMs: Vicuna-7B-v1.5 (Berkeley et al., 2023), LLaMA-2-7B-chat (Touvron et al., 2023), and StableBeluga-7B (Mahan et al.) for our experiments. These models all have 32 layers, and in the experiment, we only scale the last 30 layers, followed Zhang et al. (2024).

Models	Methods	First	Middle	Last	Avg.
		MDQA			
Vicuna-7B-v1.5	Baseline	70.0	55.6	60.2	61.9
	PI	70.6	59.6	59.8	63.3
	Ms-PoE	71.8	62.8	60.0	64.8
	Ours	70.8	61.6	61.4	64.6
StableBeluga-7B	Baseline	68.8	58.8	70.8	66.1
	PI	72.0	58.8	69.4	66.7
	Ms-PoE	73.0	59.4	64.0	65.5
	Ours	72.0	62.0	71.0	68.3
Key-Value Retrieval					
Vicuna-7B-v1.5	Baseline	95.5	55.5	73.5	74.8
	PI	98.0	90.5	84.0	90.8
	Ms-PoE	97.5	69.5	72.5	79.8
	Ours	99.0	95.0	90.5	94.8
StableBeluga-7B	Baseline	90.5	6.00	81.50	51.0
	PI	94.0	22.5	83.5	66.1
	Ms-PoE	89.5	34.0	77.5	67.0
	Ours	98.5	37.0	87.0	68.33

Table 2: “First”, “Middle”, and “Last” indicate that the correct document is located at the beginning, middle, and end of the context.

MDQA (Liu et al., 2024d) is a multi-document question-answering dataset. Due to the context window limitations of LLMs, we selected 10 documents as context and evaluated the model’s answer accuracy when the correct document appeared at different positions. Key-Value Retrieval dataset (Liu et al., 2024d) consists of key-value pairs where

both keys and values are UUIDs, enabling an assessment of the model’s retrieval capability across different positions without semantic interference. ZeroSCROLLS (Shaham et al., 2023) includes multiple long-text task datasets. we selected seven sub-datasets: GovReport, SummScreenFD, Qasper, QMSum, NarrativeQA, SQuALITY, and SpaceDigest to evaluate the model’s performance in summarization, question answering, and comprehension under long-context scenarios. We set the context window to 3,500 tokens and limit the maximum number of decoded tokens to 500.

In table 2, PI represents the scaling factor for each layer is the same, and its value is the average of the layer-specific scaling factors. Ms-PoE dynamically assigns scale factors ranging from 1.2 to 11.8 to the heads based on their sensitivity to relevant information across all layers. The more sensitive an attention head is to relevant information, the smaller the scaling factor assigned to it.

Result: We primarily discuss our experimental results from three aspects: performance, generalization, and efficiency.

I. Dynamic scaling factor allocation based on layer characteristics enhances contextual utilization:

As shown in Table 2, our method mitigates the “lost-in-the-middle” phenomenon while maintaining performance at context both ends. Compared to baselines, it achieves consistent gains, most notably a 20.0-point improvement on Key-Value Retrieval. In contrast, uniform scaling across layers (e.g., PI and Ms-PoE) improves mid-context utilization but impairs information retrieval from context both ends. On MDQA, both PI and Ms-PoE degrade performance at end positions, underscoring the necessity of layer-specific scaling.

Across multiple long-text tasks of Table 6 in the Appendix, all three models showed overall improvements, ranging from 1.66 to 2.44.

Notably, Vicuna-7B-v1.5 demonstrated an improvement of 10.55 on the Qasper dataset. This demonstrates that incorporating a layer-specific scaling method can significantly enhance the model’s utilization of contextual information.

II. Our systematic search algorithm efficiently identifies layer-specific scaling factors across models with minimal data.

While Ms-PoE (Zhang et al., 2024) manually tailors scaling factors for Vicuna, this approach fails to generalize: transferred to StableBeluga-7B (Mahan

et al.), it degrades end-position performance by 6.8% on MDQA. Moreover, Ms-PoE lacks a systematic scaling factors selection framework. By contrast, our method identifies optimal layer-specific scaling factors for diverse models using only 10% data on MDQA. For instance, it determines optimal scaling factors for Vicuna-7B-v1.5 (Berkeley et al., 2023) in 6 hours on four A100 GPUs with MDQA, demonstrating both efficiency and generalizability.

III. Our method does not introduce any delay to the model’s inference speed. Ms-PoE (Zhang et al., 2024) requires real-time calculation of each head’s sensitivity to relevant information, and different scaled positional encoding must be assigned individually to each attention head across almost all layers, which results in a decrease in inference speed. Using one 3090 GPU, we measured the average inference time per sample for the Vicuna-7B-v1.5 on the MDQA dataset. For Ms-PoE, the inference time per sample is 4.4 seconds, while our method requires only 3.1 seconds, which is roughly faster 30%, making our approach more efficient.

4.2 Enhanced Extrapolation Ability of the Model

Experimental Setup: Vicuna-7B-v1.5 (Berkeley et al., 2023) and LLaMA-2-7B-hf (Touvron et al., 2023), both with a 4K context window, were used to conduct experiments on 100 samples extracted from the validation set of the PG19 dataset (Rae et al., 2019) to validate the effectiveness of layer-specific positional encoding scaling in improving the model’s long-text extrapolation capability. Perplexity (PPL) at sequence lengths of 5K, 6K, 7K, and 8K is used to assess the extrapolation ability of model. If the extrapolation length is L' and the model’s context window size is L , we define the scaling factor as

$$s = \frac{L'}{L} \quad (13)$$

To explore the advantages of layer-specific positional encoding, we introduced an interval of 0.3, allowing the scale to vary between the minimum value s and the maximum value $s + 0.3$. As the layer index increases, the scaling factor first increases linearly to its maximum value and then decreases linearly back to its minimum value. The rationale behind this varying trend is discussed in detail in the Discussion section 5.

PI (Chen et al., 2023a) extends the context window by scaling position indices, and Dynamic-NTK (LocalLLaMA, 2023) extends it by scaling the base of positional encoding. These methods apply uniform scaling across all layers of the model, overlooking the characteristics of layers. We set the scaling factor of PI and Dynamic-NTK as the average of the layer-specific scaling factors set: $s + 0.15$ and is applied to every layer of the model to investigate whether layer-specific positional encoding scaling can improve the performance of these methods.

Result: In table 3, Layer-specific scaling method achieves lower perplexity across various methods and extrapolation lengths. When the context window exceeds the pretrained length, the out-of-distribution (OOD) issue (Jin et al., 2024) arises in attention distribution across the model’s layers. PI, Dynamic-NTK, and various extrapolation techniques can restore the attention distribution to normal, but the sensitivity to OOD issues varies across layers, suggesting that the scaling factor should differ for each layer.

Model	Method	5k	6k	7k	8k
LLaMA-2-7B-hf	PI	7.306	8.619	9.507	10.41
	Ours-PI	7.075	8.366	9.365	10.28
	Dy-NTK	6.947	7.814	8.703	9.507
	Ours-Dy-NTK	6.945	7.777	8.694	9.499
Vicuna-7B-v1.5	PI	8.662	10.28	11.76	12.97
	Ours-PI	8.559	10.03	11.56	12.87
	Dy-NTK	8.467	9.609	10.67	11.66
	Ours-Dy-NTK	8.478	9.598	10.57	11.61

Table 3: Perplexity of 100 samples on PG19 Validate datasets. This further confirms that the layer-specific scaling method outperforms uniformed scaling(PI, Dy-NTK) in improving the model’s extrapolation capability.

5 Discussion

Attention entropy reflects the degree of focus in the model’s attention and is calculated as follows:

$$H = - \sum_{i=1}^n p_i \log p_i \quad (14)$$

where p_i is the normalized attention score for the i -th token. A smaller entropy value indicates that the model’s attention is more focused.

In Figure 8, when the model extrapolates beyond the pre-trained context window size, we observe a significant increase in the model’s attention entropy, as shown in Figure 8(a). Through interpolation, the attention entropy is reduced and approaches a normal distribution, as shown in Figure 8(b). However, Whether within or beyond the pretraining window,

as the scaling factor increases, the attention entropy first *rises and then falls*, reflecting a shift from concentrated to more dispersed attention, as shown in Figure 8(b), (c).

As shown in Figure 9 and Figure 10 in the Appendix, the scaling factors for the earlier and middle layers are relatively large, while the scaling factors for the later layers are smaller. Larger scaling factors tend to disperse the attention across more tokens, allowing the model to capture a broader context, while smaller scaling factors help to concentrate the attention on more relevant tokens, filtering out irrelevant information. Based on this observation, we hypothesize that the earlier layers play a key role in aggregating information, while the later layers specialize in filtering and refining the most pertinent information. We further suggest that larger scales provide the model with a broader perspective, while smaller scales enable the model to focus more sharply on the information most relevant to the query, minimizing interference from irrelevant data.

Additionally, our analysis revealed that attention entropy in middle layers is comparatively lower than in the model’s initial and final layers. This reduced entropy suggests that middle-layer attention mechanisms exhibit heightened sensitivity to entropy fluctuations during extrapolation. We hypothesize that strategically assigning larger scaling factors to these middle layers during interpolation could strengthen the model’s extrapolation capabilities by stabilizing their attention variation. To validate these insights, we intend to pursue rigorous empirical studies and theoretical analyses in subsequent research.

6 Conclusion

In this paper, we addressed the “lost-in-the-middle” problem that has hindered the performance of LLMs in long-context tasks. Through our proposed layer-specific positional encoding scaling method, we demonstrated a novel approach that alleviates this issue by assigning distinct scaling factors to each layer, effectively slowing down the long-term decay rate of RoPE. We also introduced an efficient genetic algorithm, constrained by Bézier curves, to determine the optimal scaling factors with minimal computational resources. This study not only advances the state of long-context modeling but also offers a practical solution that can be readily applied to various large language models.

Limitations

Due to computational resource constraints, we did not conduct experiments on models larger than 7B. However, the consistent performance improvements observed across multiple 7B models confirm the effectiveness of our method.

Although some current LLMs do not have serious “lost-in-the-middle” issue, due to their tricks on post-training with a lot data and compute resources, which is orthogonal to our method. Thus, we do not explore these models in this paper.

Additionally, given the high time complexity of the genetic algorithm, we did not carefully set its hyperparameters. Therefore, the experimental results presented in this paper may not represent the optimal performance of our approach.

References

Shengnan An, Zexiong Ma, Zeqi Lin, Nanning Zheng, and Jian-Guang Lou. 2024. Make your llm fully utilize the context. *arXiv preprint arXiv:2404.16811*.

Adam W Bargteil and Elaine Cohen. 2014. Animation of deformable bodies with quadratic b閦ier finite elements. *ACM Transactions on Graphics (TOG)*, 33(3):1–10.

UC Berkeley, Stanford Cmu, and UC San. 2023. Vicuna: An open-source chatbot impressing gpt-4 with 90quality.

Shouyuan Chen, Sherman Wong, Liangjian Chen, and Yuandong Tian. 2023a. Extending context window of large language models via positional interpolation. *arXiv preprint arXiv:2306.15595*.

Yuhan Chen, Ang Lv, Ting-En Lin, Changyu Chen, Yuchuan Wu, Fei Huang, Yongbin Li, and Rui Yan. 2023b. Fortify the shortest stave in attention: Enhancing context awareness of large language models for effective tool use. *arXiv preprint arXiv:2312.04455*.

Kevin Clark, Minh-Thang Luong, QuocV. Le, and ChristopherD. Manning. 2020. Electra: Pre-training text encoders as discriminators rather than generators. *arXiv: Computation and Language,arXiv: Computation and Language*.

Yiran Ding, Li Lyna Zhang, Chengruidong Zhang, Yuanyuan Xu, Ning Shang, Jiahang Xu, Fan Yang, and Mao Yang. 2024. Longrope: Extending llm context window beyond 2 million tokens. *arXiv preprint arXiv:2402.13753*.

Abhimanyu Dubey, Abhinav Jauhri, Abhinav Pandey, Abhishek Kadian, Ahmad Al-Dahle, Aiesha Letman, Akhil Mathur, Alan Schelten, Amy Yang, Angela Fan, et al. 2024. The llama 3 herd of models. *arXiv preprint arXiv:2407.21783*.

Xiachong Feng, Xiaocheng Feng, and Bing Qin. 2021. A survey on dialogue summarization: Recent advances and new frontiers. *arXiv preprint arXiv:2107.03175*.

Agung Haryono. 2014. Studi pembentukan huruf font dengan kurva bezier. *Teknika*, 3(1):69–78.

Junqing He, Kunhao Pan, Xiaoqun Dong, Zhuoyang Song, LiuYiBo LiuYiBo, Qianguosun Qianguosun, Yuxin Liang, Hao Wang, Enming Zhang, and Jiaxing Zhang. 2024. Never lost in the middle: Mastering long-context question answering with position-agnostic decompositional training. In *Proceedings of the 62nd Annual Meeting of the Association for Computational Linguistics (Volume 1: Long Papers)*, pages 13628–13642.

Cheng-Yu Hsieh, Yung-Sung Chuang, Chun-Liang Li, Zifeng Wang, Long T Le, Abhishek Kumar, James Glass, Alexander Ratner, Chen-Yu Lee, Ranjay Krishna, et al. 2024. Found in the middle: Calibrating positional attention bias improves long context utilization. *arXiv preprint arXiv:2406.16008*.

Zhiheng Huang, Davis Liang, Peng Xu, and Bing Xiang. 2020. Improve transformer models with better relative position embeddings. *arXiv preprint arXiv:2009.13658*.

Hongye Jin, Xiaotian Han, Jingfeng Yang, Zhimeng Jiang, Zirui Liu, Chia-Yuan Chang, Huiyuan Chen, and Xia Hu. 2024. Llm maybe longlm: Self-extend llm context window without tuning.

Zhenzhong Lan, Mingda Chen, Sebastian Goodman, Kevin Gimpel, Piyush Sharma, and Radu Soricut. 2019. Albert: A lite bert for self-supervised learning of language representations. *arXiv: Computation and Language,arXiv: Computation and Language*.

Jiaqi Li, Mengmeng Wang, Zilong Zheng, and Muhan Zhang. 2023. Loogle: Can long-context language models understand long contexts? *arXiv preprint arXiv:2311.04939*.

Ming Li, Yanhong Li, and Tianyi Zhou. 2024a. What happened in llms layers when trained for fast vs. slow thinking: A gradient perspective. *arXiv preprint arXiv:2410.23743*.

Tianle Li, Ge Zhang, Quy Duc Do, Xiang Yue, and Wenhui Chen. 2024b. Long-context llms struggle with long in-context learning. *arXiv preprint arXiv:2404.02060*.

Aixin Liu, Bei Feng, Bing Xue, Bingxuan Wang, Bochao Wu, Chengda Lu, Chenggang Zhao, Chengqi Deng, Chenyu Zhang, Chong Ruan, et al. 2024a. Deepseek-v3 technical report. *arXiv preprint arXiv:2412.19437*.

Jiawei Liu, Chunqiu Steven Xia, Yuyao Wang, and Lingming Zhang. 2024b. Is your code generated by chatgpt really correct? rigorous evaluation of large language models for code generation. *Advances in Neural Information Processing Systems*, 36.

Nelson F Liu, Kevin Lin, John Hewitt, Ashwin Paranjape, Michele Bevilacqua, Fabio Petroni, and Percy Liang. 2024c. Lost in the middle: How language models use long contexts. *Transactions of the Association for Computational Linguistics*, 12:157–173.

Nelson F Liu, Kevin Lin, John Hewitt, Ashwin Paranjape, Michele Bevilacqua, Fabio Petroni, and Percy Liang. 2024d. Lost in the middle: How language models use long contexts. *Transactions of the Association for Computational Linguistics*, 12:157–173.

LocalLLaMA. 2023. *Dynamically scaled rope further increases performance of long context llama with zero fine-tuning*.

Dakota Mahan, Ryan Carlow, Louis Castricato, Nathan Cooper, and Christian Laforte. *Stable beluga models*.

Xin Men, Mingyu Xu, Qingyu Zhang, Bingning Wang, Hongyu Lin, Yaojie Lu, Xianpei Han, and Weipeng Chen. 2024. Shortgpt: Layers in large language models are more redundant than you expect. *arXiv preprint arXiv:2403.03853*.

Yves Mineur, Tony Lichah, Jean Marie Castelain, and Henri Giaume. 1998. A shape controled fitting method for b  zier curves. *Computer Aided Geometric Design*, 15(9):879–891.

M.E. Mortenson. 1999. *Mathematics for Computer Graphics Applications*. G - Reference,Information and Interdisciplinary Subjects Series. Industrial Press.

Alexander Peysakhovich and Adam Lerer. 2023. Attention sorting combats recency bias in long context language models. *arXiv preprint arXiv:2310.01427*.

JackW. Rae, Anna Potapenko, SiddhantM. Jayakumar, and TimothyP. Lillicrap. 2019. Compressive transformers for long-range sequence modelling. *arXiv: Learning,arXiv: Learning*.

Uri Shaham, Maor Ivgi, Avia Efrat, Jonathan Berant, and Omer Levy. 2023. Zeroscrolls: A zero-shot benchmark for long text understanding.

Peter Shaw, Jakob Uszkoreit, and Ashish Vaswani. 2018. Self-attention with relative position representations. *arXiv preprint arXiv:1803.02155*.

Jianlin Su, Murtadha Ahmed, Yu Lu, Shengfeng Pan, Wen Bo, and Yunfeng Liu. 2024. Roformer: Enhanced transformer with rotary position embedding. *Neurocomputing*, 568:127063.

Jianlin Su, Yu Lu, Shengfeng Pan, Bo Wen, and Yunfeng Liu. 2021. Roformer: Enhanced transformer with rotary position embedding. *Cornell University - arXiv,Cornell University - arXiv*.

Qi Sun, Marc Pickett, Aakash Kumar Nain, and Llion Jones. 2024. Transformer layers as painters. *arXiv preprint arXiv:2407.09298*.

Gemini Team, Petko Georgiev, Ving Ian Lei, Ryan Burnell, Libin Bai, Anmol Gulati, Garrett Tanzer, Damien Vincent, Zhufeng Pan, Shibo Wang, et al. 2024. Gemini 1.5: Unlocking multimodal understanding across millions of tokens of context. *arXiv preprint arXiv:2403.05530*.

Hugo Touvron, Louis Martin, Kevin Stone, Peter Albert, Amjad Almahairi, Yasmine Babaei, Nikolay Bashlykov, Soumya Batra, Prajwala Bhargava, Shruti Bhosale, et al. 2023. Llama 2: Open foundation and fine-tuned chat models. *arXiv preprint arXiv:2307.09288*.

Yusen Zhang, Ansong Ni, Ziming Mao, Chen Henry Wu, Chenguang Zhu, Budhaditya Deb, Ahmed H Awadallah, Dragomir Radev, and Rui Zhang. 2021. Summ^ n: A multi-stage summarization framework for long input dialogues and documents. *arXiv preprint arXiv:2110.10150*.

Zhenyu Zhang, Runjin Chen, Shiwei Liu, Zhewei Yao, Olatunji Ruwase, Beidi Chen, Xiaoxia Wu, and Zhangyang Wang. 2024. Found in the middle: How language models use long contexts better via plug-and-play positional encoding. *arXiv preprint arXiv:2403.04797*.

Ling Zheng, Pengyun Zeng, Wei Yang, Yinong Li, and Zhenfei Zhan. 2020. B  zier curve-based trajectory planning for autonomous vehicles with collision avoidance. *IET Intelligent Transport Systems*, 14(13):1882–1891.

Qinkai Zheng, Xiao Xia, Xu Zou, Yuxiao Dong, Shan Wang, Yufei Xue, Zihan Wang, Lei Shen, Andi Wang, Yang Li, et al. 2023. Codegeex: A pre-trained model for code generation with multilingual evaluations on humaneval-x. *corr abs/2303.17568 (2023)*. *arXiv preprint arXiv:2303.17568*, 10.

A Exploring layer-wise characteristics

Layers operated on	First	Middle	Last
Baseline			
—	68.33	60.30	64.33
2 layers			
2,3	68.00	60.33	63.67
4,5	68.33	59.67	64.67
6,7	67.00	59.33	62.67
8,9	63.33	64.33	65.60
9,10	65.67	61.00	64.33
11,12	68.67	60.00	62.67
13,14	70.33	63.33	66.33
15,16	69.33	57.67	63.33
17,18	68.67	59.33	64.33
19,20	69.00	60.00	64.33
21,22	70.33	61.33	64.33
23,24	69.00	61.33	64.33
25,26	68.67	61.33	64.33
27,28	68.33	60.67	64.67
29,30	69.00	59.00	63.67
3 layers			
2,3,4	68.00	59.00	61.67
5,6,7	68.33	59.33	66.00
8,9,10	59.67	64.00	66.33
10,11,12	68.33	59.67	62.67
13,14,15	71.00	63.33	64.67
16,17,18	68.33	58.67	64.00
19,20,21	71.00	58.33	65.67
22,23,24	70.00	62.67	63.67
25,26,27	67.67	61.00	64.67
28,29,30	70.67	61.00	63.33
4 layers			
2,3,4,5	68.67	59.00	64.33
6,7,8,9	61.00	61.33	68.33
10,11,12,13	65.33	58.00	61.00
14,15,16,17	68.67	61.00	67.00
18,19,20,21	70.67	58.67	65.33
22,23,24,25	71.00	62.67	66.00
25,26,27,28	70.33	61.67	64.33

Table 4: The impact of scaling layers at different positions on the results. The three largest values at context ends were highlighted in blue.

We selected the first 300 samples from the MDQA dataset (Liu et al., 2024d) and set the scaling factor to 1.6. To investigate how scaling layers at different positions impacts the utilization of context at both ends, we applied uniform scaling factors to consecutive layers of **Vicuna-7B-v1.5** (Berkeley et al., 2023) at different positions, ensuring that other layers were unaffected. The results show that scaling

the earlier layers enhances the model’s focus on the latter parts of the context, whereas scaling the later layers shifts the model’s attention to the earlier contextual information. These findings suggest that different layers exhibit distinct characteristics, with variations in how they process and attend to different positions within the context.

B Dataset

We used the MDQA and Key-Value Retrieval datasets (Liu et al., 2024c) to investigate the effectiveness of our method in alleviating the “lost-in-the-middle” issue. The corresponding prompt templates for these datasets are shown in Figure 6 and Figure 7. Building upon these experiments, we further examined whether addressing this issue could enhance the model’s ability to leverage contextual information by testing it on the ZeroScroll dataset (Shaham et al., 2023). A detailed description of the dataset and the evaluation metrics used can be found in Table 5. We use the first 200 samples of the MDQA dataset to determine the scaling factors and the last 500 samples for the “lost-in-the-middle” test. For the Key-Value Retrieval dataset, we use 200 samples for scaling factors tuning and 200 samples for the “lost-in-the-middle” test.

Write a high-quality answer for the given question using only the provided search results (some of which might be irrelevant).
{search_results}
Question: {question}
Answer:

Figure 6: The prompt template of MDQA dataset.

Extract the value corresponding to the specified key in the JSON object below.
JSON data:
{formatted_kv_records}
Key: “[key]”
Corresponding value:

Figure 7: The prompt template of Key-Value Retrieval dataset.

Dataset	Description	Metric
GovReport	Summarization of long reports.	Geometric mean of Rouge-1/2/L scores
SummScreenFD	Summarization of TV shows episodes scripts.	Geometric mean of Rouge-1/2/L scores
QMSum	Query-based summarization over meeting transcripts.	Geometric mean of Rouge-1/2/L scores
SQuALITY	Question-focused summarization over stories.	Geometric mean of Rouge-1/2/L scores
Qasper	Question answering over research papers.	F1 score
NarrativeQA	Question answering about entire books and movie scripts.	F1 score
SpaceDigest	Aggregated sentiment classification over 50 hotel reviews from Space.	Exp_similarity

Table 5: Introduction and evaluation metrics of the sub-datasets under ZeroScroll.

Model	Method	GovReport	Qasper	SummScreenFd	Qmsum	NarrativeQA	Squality	SpaceDigest	Average
Vicuna-7B-v1.5	Baseline	18.44	22.82	13.71	14.50	10.98	16.56	21.39	16.91
	Ours	21.47	33.37	14.39	15.53	11.52	16.91	22.24	19.35
LLaMA-2-7B-chat	Baseline	18.00	13.48	13.73	14.29	10.28	15.94	49.72	19.35
	Ours	18.20	15.23	13.99	15.04	14.93	17.37	52.28	21.01
StableBeluga-7B	Baseline	14.88	26.89	12.09	14.24	10.73	15.05	48.50	20.34
	Ours	18.98	34.19	13.06	15.46	9.91	16.65	46.61	22.12

Table 6: Our method showed improvements across multiple models on seven long-text tasks, demonstrating its effectiveness in enhancing the model’s ability to utilize contextual information. Descriptions and evaluation metrics of datasets are provided in Table 5.

C Enhance the utilization of long context

We further explore the performance of our method in various long-context tasks, as shown in Table 5.

D Discussion Details

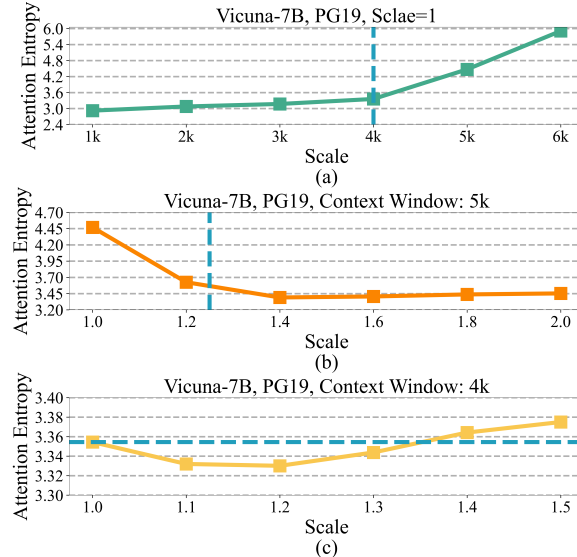


Figure 8: Figure (a) shows that as input length exceeds the pre-training context window (4k), attention entropy increases. Figure (b) illustrates that in a 5k window, attention entropy first decreases and then increases with interpolation strength, where the blue line marks the normal strength ($5k/4k = 1.25$). Figure (c) demonstrates that within the pre-training window, smaller scales concentrate attention while larger scales disperse it.

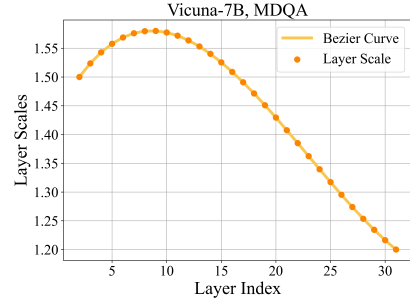


Figure 9: On the MDQA dataset, Bézier curves determined for Vicuna-7B-v1.5 using a genetic algorithm allocated larger scaling factors to the earlier layers and smaller scaling factors to the later layers..

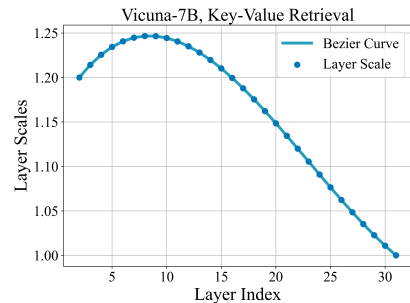


Figure 10: On the Key-Value Retrieval dataset, Bézier curves determined for Vicuna-7B-v1.5 using a genetic algorithm allocated larger scaling factors to the earlier layers and smaller scaling factors to the later layers.